Chemical Engineering Journal 541 (2026) 177653

Contents lists available at ScienceDirect

Chemical Engineering Journal

journal homepage: www.elsevier.com/locate/cej

Carbonic anhydrase boosts multi-step CO_2 conversion: A synergistic approach of co-immobilized enzymes for CO_2 valorization

Sady Roberto Rodriguez [a], Ayanne De Oliveira Maciel [b], Oscar Romero [a], Marina Guillén [a,*], Io Antonopoulou [b,**]

[a] Bioprocess Engineering and Applied Biocatalysis Group (ENG4BIO), Department of Chemical, Biological and Environmental Engineering, Universitat Autònoma de Barcelona, 08193, Bellaterra, Spain

[b] Biochemical Process Engineering, Division of Chemical Engineering, Department of Civil, Environmental and Natural Resources Engineering, Luleå University of Technology, 97187, Luleå, Sweden

ARTICLE INFO

Dataset link: Replication data for "Carbonic anhydrase boosts multi-step CO2 conversion: A synergistic approach of co-immobilized enzymes for CO2 valorization" (Original data)

Keywords:
CO_2 hydration
Carbonic anhydrase
Carbon capture and utilization
Multi-enzymatic system
Gas-liquid transfer
Co-immobilization

ABSTRACT

Carbon dioxide (CO_2) is an underutilized industrial byproduct whose conversion into valuable molecules is mainly constrained by slow gas–liquid transfer. Carbonic anhydrase (CA) efficiently accelerates CO_2 hydration to bicarbonate, increasing its availability in the liquid phase. Therefore, integrating CA into CO_2 bioconversion processes is a promising strategy for Carbon Capture and Utilization (CCU). This study investigates CA's role in enhancing CO_2 mass transfer in a multi-enzymatic platform comprising the co-immobilized formate dehydrogenase (FDH) for CO_2 reduction to formate and glycerol dehydrogenase (GlyDH) for in situ NADH regeneration via glycerol oxidation to dihydroxyacetone (DHA). Three microbial CA variants were screened, identifying *Bacillus halodurans* CA (BhCA) as the best candidate due to boosted formate production, immobilization on Ni^{2+}-ReliZyme, and operational stability. Consequently, a novel trifunctional biocatalyst was rationally prepared from crude cell lysates using a one-step purification / co-immobilization strategy, enabling controlled enzyme incorporation at optimal activity ratios and yielding a streamlined, cost-effective, and industrially relevant biocatalyst with high catalytic performance. In the reaction, BhCA significantly enhanced CO_2 reduction to formate by FDH, increasing yield by up to 1.8-fold and reaction rate by up to 4.3-fold. This synergy with FDH arises from CA-mediated stabilization of the CO_2–bicarbonate interconversion, which enhances gas–liquid transfer and promotes CO_2 reduction. Reusability tests showed remarkable stability with BhCA retaining 63.5 ± 0.8% of its activity and achieving 80.3 ± 1.9% formate yield after five cycles. Overall, CA acts as an effective intensifier for bio-based CCU, boosting both CO_2 capture and its conversion into high-value products within multi-enzymatic platforms.

1. Introduction

Carbon dioxide (CO_2) is an underutilized byproduct emitted by various industrial sources, and its accumulation in the atmosphere poses significant risks to human health and environment [1]. Significant efforts have focused on mitigating it through carbon capture and utilization (CCU) strategies to convert it into value-added compounds. However, these processes face major bottlenecks due to the high thermodynamic stability of CO_2 and its slow transfer across the gas–liquid interface [2]. To address these challenges, several reactor and process design strategies have been explored, including gas-contact membranes, micro- and nanobubble technologies, and liquid-phase chemical adsorbents such as amines and carbonates. However, their broad application has been hindered by low selectivity and efficiency, along with high complexity and energy requirements [3].

Within this framework, carbonic anhydrase (CA) is among the most abundant and catalytically efficient enzymes in nature, facilitating the rapid hydration of CO_2 to bicarbonate (HCO_3^-) across multiple cellular metabolic pathways [4]. CA is a zinc-containing metalloenzyme with turnover frequencies up to 10^6 s^{-1} that lowers the activation energy for

* Correspondence to: M. Guillén, Department of Chemical, Biological and Environmental Engineering, Universitat Autònoma de Barcelona, 08193, Bellaterra, Catalonia, Spain.

** Correspondence to: I. Antonopoulou, Department of Civil, Environmental and Natural Resources Engineering, Luleå University of Technology, Luleå, Sweden.
E-mail addresses: Marina.Guillen@uab.cat (M. Guillén), io.antonopoulou@ltu.se (I. Antonopoulou).

https://doi.org/10.1016/j.cej.2026.177653
Received 9 February 2026; Received in revised form 19 May 2026; Accepted 22 May 2026
Available online 23 May 2026
1385-8947/© 2026 The Authors. Published by Elsevier B.V. This is an open access article under the CC BY license (http://creativecommons.org/licenses/by/4.0/).

CO_2 hydration through metal-assisted deprotonation of a water molecule [5]. This high catalytic efficiency enhances the liquid's capacity to absorb CO_2, promoting its transfer from the gas to the liquid phase and subsequent conversion into a more stable species in solution, bicarbonate [6]. The reaction mechanism can be summarized by the following two equations:

$$CO_{2\,(g)} \leftrightarrow CO_{2\,(aq)} \quad (1)$$

$$CO_{2\,(aq)} + H_2O \leftrightarrow HCO_3^- + H^+ \quad (2)$$

Due to these catalytic properties, CA stands out as an excellent tool for deploying bio-based CCU processes, facilitating not only the initial CO_2 capture / solubilization stage but also the subsequent transformation by biocatalytic, electrocatalytic, photocatalytic, and thermocatalytic processes [2]. The role of CA has been extensively studied in conjunction with formate dehydrogenase (FDH) for the CO_2 reduction to formate [7,8], coupled with NADH consumption. FDH is a strategically important biocatalyst for climate change mitigation and circular bioeconomy, enabling the production of formate (or formic acid), a versatile and industrially relevant product as an energy carrier and chemical building block [9]. The synergy between CA and FDH has resulted in significant improvements in both reaction rate and formate yields [10–12]. In addition, this performance is strongly influenced by the pH of the medium and the distribution of inorganic carbon species from CO_2 dissolution, with CA acting as a critical mediator of CO_2 hydration, enhancing its availability in the liquid phase. Despite these achievements in enzyme synergy, the optimization of CA to enhance CO_2 gas–liquid transfer in CCU systems for formate production by FDH remains largely unexplored, particularly in terms of its impact on reaction efficiency and scalability within multi-enzymatic platforms.

To support this approach, several microbial CA variants have shown outstanding performance in multi-step CO_2 capture and fixation due to their high thermostability and broad pH tolerance under moderate pressure conditions [13]. Furthermore, CA immobilization on solid supports has been demonstrated to significantly prolong lifespan, improve reusability and recovery, and reduce overall costs [14]. This strategy may enhance CA robustness under industrial conditions, making it highly appealing for practical CCU applications [15]. However, although several enzymatic CCU systems employing CA have been reported in recent years, most studies have mainly focused on binary CA–FDH cascades designed to enhance CO_2 hydration and improve formate synthesis efficiency. In general, these systems rely on purified enzymes, are limited to the production of a single target compound [7,10,12], and rarely address key aspects required for industrial implementation, such as simplified biocatalyst preparation, integrated cofactor regeneration, operation under realistic gas compositions, and long-term operational stability [2,16–18]. In addition, the role of CA has predominantly been evaluated only in terms of accelerating CO_2 hydration, while its broader impact within more complex multienzyme catalytic networks remains largely unexplored [19]. A similar limited functional role has also been observed in other CO_2 conversion technologies, such as electrochemical and photocatalytic systems, where CA is mainly used to enhance CO_2 availability at the reaction interface rather than being exploited as a strategic component for reaction engineering improvement [11,20–22]. Therefore, the development of robust, sustainable and industrially relevant multienzyme platforms capable of simultaneously integrating CO_2 capture enhancement, long-term operation, and multi-product synthesis still represents an important challenge in enzymatic CCU technologies.

This study introduces a novel trifunctional biocatalyst that enhances CO_2 reduction to formate by integrating carbonic anhydrase (CA) into a multi-enzymatic platform for the production of high-value compounds (Fig. 1). The original system comprises the multi-enzymatic co-production of formate from CO_2 by formate dehydrogenase (FDH), followed by in situ NADH cofactor regeneration through glycerol oxidation to dihydroxyacetone (DHA) catalyzed by glycerol dehydrogenase (GlyDH) as a recycling enzyme. In contrast to conventional cofactor regeneration strategies, the use of GlyDH not only sustains cofactor turnover but also enables the simultaneous production of an additional high-value industrial compound, DHA. This platform has been previously optimized using both free enzymes [23] and co-immobilized enzymes (bifunctional biocatalyst) on a Ni^{2+}-ReliZyme carrier, resulting in a remarkably high

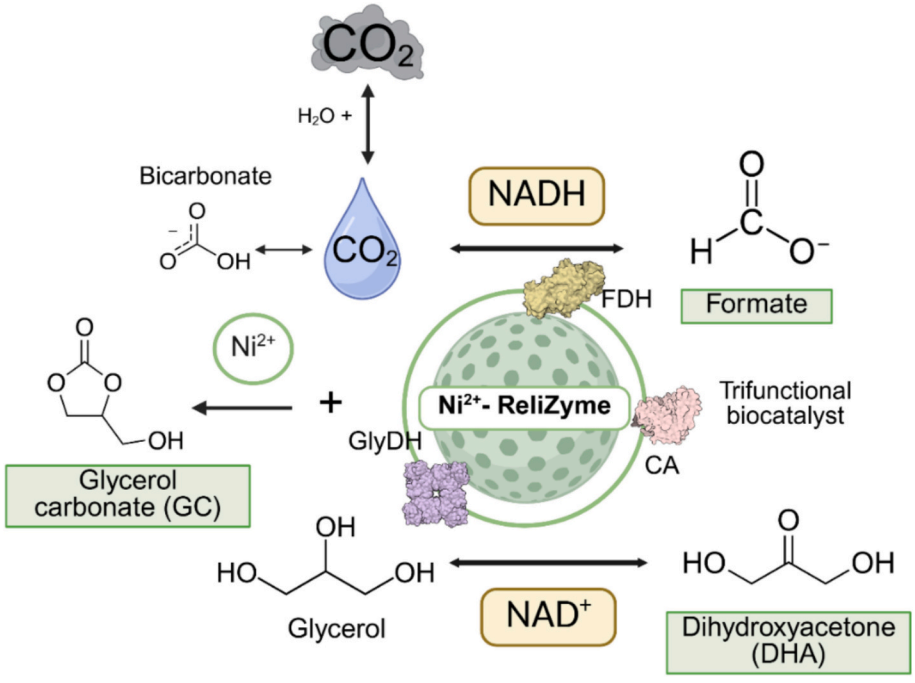

Fig. 1. Multi-enzymatic CO_2 reduction system for the production of high-value compounds, assisted by carbonic anhydrase (CA). The system combines CO_2 hydration by CA with its subsequent reduction to formate catalyzed by formate dehydrogenase (FDH). In situ NADH regeneration is achieved through glycerol oxidation to dihydroxyacetone (DHA) by glycerol dehydrogenase (GlyDH). Additionally, glycerol carbonate (GC) is produced as a byproduct via a metal-catalyzed reaction between CO_2 and glycerol.

formate concentration enabled by optimized, reactor-engineered continuous CO_2 supplementation and aligned with green metrics [24,25]. Additionally, glycerol carbonate (GC) is formed as a byproduct via the direct carboxylation of glycerol with CO_2 (reaction mechanism in Fig. S9 in Supplementary Information [SI]) catalyzed by the nickel functionalized on the Ni^{2+} -ReliZyme carrier and the zinc (Zn^{2+}) from the metalloenzyme glycerol dehydrogenase from *Bacillus stearothermophilus* used in this study [26]. As a result, an additional high-value industrial compound is generated, thereby enhancing the system's attractiveness for potential applications.

For this work, CA was incorporated via a rationally designed trifunctional biocatalyst prepared on the same carrier, based on an initial screening of three microbial CA variants. Importantly, the trifunctional derivative was generated directly from crude cell lysates, enabling a more streamlined, cost-effective, and industrially relevant preparation of the co-immobilized system compared to conventional multistep immobilization approaches. Accordingly, the contribution of CA-catalyzed CO_2 hydration was evaluated within the multi-enzymatic system, not only in relation to formate production but also regarding its effect on the coupled synthesis of DHA and glycerol carbonate, together with its operational stability and reusability over multiple reaction cycles. This represents a clear example of an integrated co-immobilized enzymatic platform within a CCU framework, in which the orchestrated activity of the enzymes simultaneously improves the reaction rate, catalytic efficiency, and product yields, driven by CA-mediated enhancement of CO_2 gas–liquid transfer, thereby boosting the efficient CO_2 capture and valorization into high-value industrial chemicals.

2. Experimental section

2.1. Materials

All chemical and reagents were purchased from Merck KGaA (Darmstadt, Germany). The cofactors NADH and NAD^+ were purchased from GERBU Biotechnik GmbH (Heidelberg, Germany). ReliZyme™ EP403S resin was purchased from Resindion S.r.l. (Binasco, Italy). The gas mixture 20% CO_2 and 80% N_2 was purchased from Linde Gas AB (Luleå, Sweden). Alexa Fluor 610-X, 488 and 405 dyes as well as Antibody Conjugate Purification kit were purchased from Thermo Fisher Scientific (Massachusetts, USA).

2.2. Enzymes production and purification

FDH from *Candida boidinii* and GlyDH from *Bacillus stearothermophilus* were produced and purified by the ENG4BIO research group according to the procedures reported by Rodriguez et al. [23]. The following microbial CA variants were produced and purified: *Aeribacillus pallidus* CA (ApCA, Genbank ID: KZM53878 [27]), *Bacillus halodurans* CA (BhCA, Genbank ID: ALI16144 [28]) and *Desulfovibrio vulgaris* CA (DvCA8.0 [29]). Briefly, CAs variants were expressed in *E. coli* BL21 using a pET22b(+) vector with a 6 × His tag. Cells were grown in Luria–Bertani (LB) and auto-induction media, then lysed, filtered, freeze-dried, and dialyzed, following the protocols detailed by De Oliveira Maciel et al [30]. CAs were purified from clarified lysate by ultrafiltration and His-tag affinity chromatography (TALON IMAC, ÄKTA system), buffer-exchanged to Tris-HCl, concentrated, and verified by SDS-PAGE and CA activity assays, according to Antonopoulou et al [31].

2.3. Enzyme activity assays

FDH and GlyDH activities were measured by NAD^+ reduction to NADH, driven by formate oxidation to CO_2 and glycerol oxidation to DHA, respectively, following the protocols detailed by Rodriguez et al [23]. For CA activity, two different activity assays were independently employed throughout this work. *Phenolphthalein assay*: CA activity was measured spectrophotometrically by monitoring CO_2 release from a bicarbonate solution using a colorimetric pH indicator (phenolphthalein), according to methodology reported by Antonopoulou et al [32]. *pNP-acetate assay*: CA activity was determined via its esterase activity by spectrophotometrically monitoring the hydrolysis of *p*-nitrophenyl acetate (pNP-acetate) to p-nitrophenol (pNP), following protocols by Murín et al [33].

2.4. Evaluation of different carbonic anhydrases (CA) in the enzymatic CO_2 reduction system

The enzymatic CO_2 reduction by FDH was evaluated by individually incorporating the three previously mentioned CA variants. Initially, the immobilization of each purified CA was performed on the Ni^{2+}-ReliZyme carrier (functionalization in protocol S2, SI) at a 1:10 carrier-to-volume ratio. Each CA solution was prepared in phosphate buffer 100 mM + NaCl 100 mM (pH 7.5) and incubated with the carrier at 4 °C for 24 h under continuous agitation. The resulting biocatalysts were filtered and washed with the same buffer. Samples were collected to measure catalytic activity in the blank, suspension, and supernatant, and protein content following SI protocols. The evaluation of the immobilized biocatalyst was based on the equations provided in the protocol S8.

For the evaluation of formate synthesis from CO_2, a co-immobilized biocatalyst with FDH and each CA was prepared with 10 mg of purified FDH and each purified CA per g of carrier. Reactions were carried out in phosphate buffer 100 mM (pH 7.5) containing 10 mM NADH, with continuous gas supplementation from a 20% CO_2 and 80% N_2 mixture at 0.1 vvm. Experiments were carried out in duplicate at 30 °C, 300 rpm and for 24 h. At the end of the reaction, formate and NADH concentrations (protocols S4 and S5, SI), as well as residual CA activity (phenolphthalein assay) were determined.

2.5. Design of a tri-enzymatic co-immobilized biocatalyst on Ni^{2+}-ReliZyme carrier

First, a bifunctional biocatalyst was prepared with GlyDH and FDH enzymes from cell lysates as a one-step purification/co-immobilization strategy via IMAC affinity immobilization between nickel and 6× His-tag, following the protocol previously reported by Rodriguez et al [24]. Briefly, GlyDH was immobilized on the Ni^{2+}-ReliZyme carrier and coated with glutaraldehyde for stabilization (GC-GlyDH). The resulting biocatalyst was then filtered and washed. Subsequently, FDH was added to the GlyDH-immobilized derivative, subsequently filtered and washed.

For the trifunctional biocatalyst, a CA solution from cells lysates was prepared in phosphate 100 mM + NaCl 100 mM buffer (pH 7.5) and subsequently incubated with the previously bifunctional biocatalyst via IMAC immobilization affinity. After 16 h of incubation, the biocatalyst was filtered and washed with the previous buffer followed by a solution containing 20 mM imidazole and 100 mM NaCl and stored at 4 °C. CA catalytic activity was determined using the phenolphthalein assay. The parameters evaluated in the co-immobilization were defined as follows (equations section S8, SI):

2.5.1. Theoretical biocatalyst activity

Maximum enzymatic activity expected for the immobilized biocatalyst, assuming that all immobilized enzymes retains their full catalytic activity after immobilization.

2.5.2. Observed biocatalyst activity

Experimentally measured enzymatic activity of the biocatalyst, reflecting the actual performance, which may be limited by diffusional or mass-transfer constraints.

2.5.3. Immobilization yield (based on activity)

Percentage of the initially offered enzymatic activity that is successfully bound to the carrier after immobilization.

2.5.4. Retained activity

Percentage of the immobilized enzymatic activity that remains catalytically active after immobilization.

2.5.5. Recovery activity

Percentage of the initially offered enzymatic activity that is recovered in the final biocatalyst.

2.6. Immobilization of BhCA on ReliZyme carriers with different activation degrees

BhCA was immobilized on ReliZyme carriers after controlled hydrolysis of epoxy groups for different time periods. Epoxy-ReliZyme carrier was incubated in hydrochloric acid (HCl) 1 M at a 1:10 solid-to-liquid ratio for 1, 2 and 4 h. The carrier without acid hydrolysis treatment was used as the control. Epoxy groups (equivalent to iminodiacetic acid (IDA) groups at a 1:1 ratio) were quantified following the protocol from Santiago-Arcos et al [34]. Briefly, vicinal diols generated after acid hydrolysis were oxidized with sodium periodate ($NaIO_4$), and the residual periodate was determined by iodometric titration with potassium iodide (KI). Epoxy / IDA content was calculated from the difference in $NaIO_4$ consumption between control and hydrolyzed carriers.

For subsequent immobilization, after hydrolysis, each carrier was filtered, washed with distilled water, and functionalized with IDA and nickel sulfate, following the protocol described in Section S2 of the SI. BhCA immobilization was performed with 2 mg g^{-1} of total protein, following procedure 2.5. The retained activity in the suspension was measured after 2 h of incubation to ensure that the total amount of offered protein had been bound to the carrier. BhCA catalytic activity was determined using the phenolphthalein assay.

2.7. Multi-enzymatic CO_2 reduction into high-value chemicals assisted by CA

The multi-enzymatic CO_2 reduction was performed by the trifunctional biocatalyst, featuring in situ NADH regeneration and continuous CO_2 supply. Reactions were carried out in phosphate buffer 100 mM (pH 7.5) as reaction medium, containing NADH 1 mM and glycerol 100 mM, with continuously gas bubbled at 0.1 vvm from the 20% CO_2 gas mixture. A total of 20 g of trifunctional biocatalyst was resuspended in a total volume of 200 mL. Experiments were conducted in duplicate at 30 °C, constant agitation at 300 rpm and during 54 and 82 h. A control experiment in the absence of CA was performed under same conditions. Samples were collected periodically to measure substrates, products (protocols in SI), and enzyme activities. CA catalytic activity was determined using the phenolphthalein assay.

2.8. Reusability of the trifunctional biocatalyst

The reusability of the trifunctional biocatalyst was tested over five consecutive cycles under the conditions described in the previous section. Biocatalyst concentration (100 g L^{-1}) was maintained by adjusting the reaction volume, with total loss below 7.3% after five cycles. After each cycle, biocatalyst was washed with phosphate buffer 100 mM (pH 7.5), using the same volume as that of the reaction mixture in each cycle. Performance metrics were calculated according to equations detailed in the protocol S9 in SI.

3. Results and discussion

3.1. Screening purified CA for integration into the multi-enzyme CO_2 reduction system

First, the most suitable CA for the multi-enzymatic system was selected based on its immobilization performance and catalytic efficiency in the CO_2 reduction. Previously optimized conditions for this multi-enzymatic platform included a pH of 7.0 and temperature of 30 °C, considering both CO_2 solubility and NADH cofactor stability [23]. The CA candidates evaluated are listed in Table 1. All CAs evaluated have an optimal pH of 7, however, their catalytic activity at 30 °C is relatively low, as their peak activity typically occurs above 60 °C, making them more suitable for CO_2 capture at elevated temperatures. BhCA showed the highest activity, reaching 39% of its maximum at 30 °C. In general, the evaluated CAs exhibit maximum activity at pH 6–10 and temperatures above 40 °C [35,36].

As a first experimental step, purified CAs were immobilized on Ni^{2+}-ReliZyme at a low total protein loading (2 mg g^{-1}). Fig. S1 in SI shows the immobilization kinetics, where complete depletion of each CA from the supernatant occurred approximately at 60 min. Interestingly, after 90 min, all CAs retained less than 10% of their total activity in the carrier suspension. Due to this, the incubation time was then extended to monitor their behavior on the carrier over time. Fig. 2 shows the immobilization kinetics based on retained activity in the suspension over 24 h. All CAs reached maximum activity after 16 h, with BhCA exhibiting the highest retained activity (43.7 ± 1.8%). After this point, a slight decrease in activity was observed. ApCA and DvCA8.0 reached 32.4 ± 1.9% and 37.1 ± 1.5% at 16 h, respectively, also showing declines afterward.

A study of CA immobilization on magnetic nanoparticles showed a similar behavior, with activity gradually increasing to a maximum (~70%) at 24 h, followed by a slight decline [37]. This may result from initial unfavorable enzyme conformation that later adjust or reorient on the carrier over time, improving active site exposure [38]. Studies have shown that immobilization can enhance CA's structural stability, but active site mobility may be limited by the method, enzyme loading, and support interactions, reducing access to the liquid film where CO_2 hydration occurs [2,39]. Therefore, immobilized CA efficiency may depend on the employed carrier.

It has been reported that immobilization of some multimeric enzymes on carriers with high functional group density can cause subunit dissociation and activity loss [40]. However, over time, partial restoration of the native conformation may occur, as seen with the evaluated CAs. To further assess whether the observed activity loss was intrinsically linked to the high density of functional groups on the Ni^{2+}-functionalized ReliZyme carrier, an additional set of experiments was performed using an alternative support bearing oxirane groups instead of Ni^{2+} functionalities, which allowed precise control over the number of reactive sites. Therefore, ReliZyme carriers with different epoxy / IDA groups density were prepared, and BhCA, showing the highest retained activity, was selected for this experiment (procedure in section S6, SI). As shown in Table 2, BhCA activity increased with decreasing surface epoxy / IDA group density, reaching a retained activity of 79.1 ± 2.7% after 2 h when immobilized on a carrier with only 72.4 ± 4.7 μmol IDA g^{-1}, representing a 57.8% reduction in functional groups relative to the control carrier (171.4 ± 3.4 μmol IDA g^{-1}). This indicates improved enzyme-carrier interaction and more favorable orientation, resulting in higher observed activity. Therefore, further reducing the degree of carrier functionalization would enable observation of the total immobilized activity of this protein (100%). However, reducing the number of

Table 1
Summary of the evaluated carbonic anhydrases (CA) enzymes and their main characterization parameters relevant to the multi-enzymatic CO_2 reduction system.

Acronym	Host	Optimal pH	Relative activity at 30 °C (%)*,**
ApCA	*Aeribacillus pallidus*	7	21.1 ± 7.6
BhCA	*Bacillus halodurans*		39.0 ± 2.3
DvCA8.0	*Desulfovibrio vulgaris*		28.9 ± 8.2

* Compared to its optimal temperature.
** CAs catalytic activity was determined using the pNP-acetate assay.

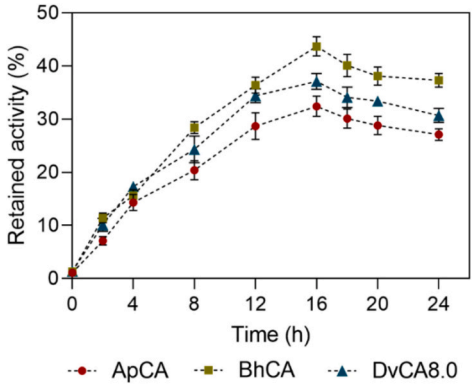

Fig. 2. Time-course of the individual immobilization of three carbonic anhydrase (CA) onto Ni^{2+}-ReliZyme carrier (2 mg g^{-1}) [retained activity over time].

Table 2
Immobilization of BhCA (2 mg g^{-1} of total protein) on ReliZyme carriers pretreated by acid hydrolysis of epoxy groups (1 M HCl, 1:10 ratio) for 1, 2, or 4 h. A non-treated carrier was used as control. BhCA catalytic activity was determined using the phenolphthalein assay.

Sample / Hydrolysis time	Retained activity (%)	Immobilization yield (%)*	IDA groups content (μmol g^{-1} carrier)
Control	12.3 ± 0.9	100 ± 0.7	171.4 ± 3.4
1 h	30.2 ± 2.6	100 ± 0.1	145.7 ± 2.9
2 h	52.5 ± 3.1	98.3 ± 1.8	118.7 ± 4.1
4 h	79.1 ± 2.7	92.1 ± 3.2	72.4 ± 4.7

* Immobilization yield based on catalytic activity.

attachment sites slightly lowered the BhCA immobilization yield from 100% to 92.1 ± 3.2%. These findings suggest that some multimeric enzymes like BhCA, and likely ApCA and DvCA8.0, can undergo catalytic site alterations on highly functionalized carriers, highlighting the need to optimize carrier surface chemistry to preserve native conformation and maximize activity.

In the literature, immobilization of CA on various carriers, such as metal nanoparticles, metal organic frameworks (MOFs), and polymeric membranes, has yielded recovered activities ranging from ~40% to 100% [41–43]. Thus, CA immobilization may depends on carrier properties, as well as on the strength and nature of enzyme–carrier interactions. Despite this, the original functionalized carrier without any chemical modification in the functional groups density will be used in the next experiments to allow co-immobilization with GC-GlyDH and FDH via nickel-affinity.

After evaluating CA immobilization, its catalytic contribution to CO_2 hydration, and the resulting enhancement of formate synthesis, was assessed using a co-immobilized biocatalyst with purified FDH and each

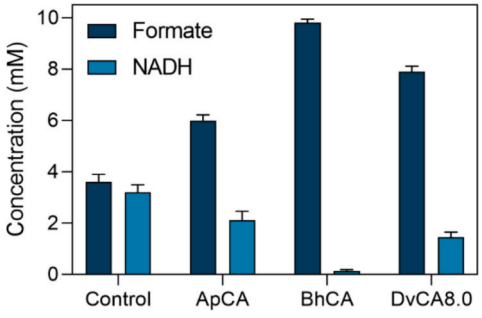

Fig. 3. Formate synthesis from CO_2 after 24 h using co-immobilized biocatalyst with FDH and CA (10 mg g^{-1} each enzyme) on Ni^{2+}-ReliZyme carrier (10 mM NADH).

CA variant (10 mg g^{-1} each enzyme). Fig. 3 shows formate production and remaining NADH after 24 h. BhCA showed the highest contribution to CO_2 solubilization, resulting in highest formate yield corresponding to 9.8 ± 0.1 mM of formate production. In addition, a nearly complete NADH consumption (97.7%) was achieved, corresponding a 2.7-fold formate increase production over the control sample. This may be related to the higher activity of immobilized BhCA (43.7 ± 1.8%) compared to ApCA and DvCA8.0, with recovered activity (Fig. 2). Formate synthesis was lower with ApCA (6.0 ± 0.3 mM) and DvCA8.0 (7.9 ± 0.2 mM) catalytic contribution; nevertheless, they still exhibited 1.7- and 2.2-fold increases in formate production compared to the control, respectively. Likewise, all CAs showed remarkable operational stability, with BhCA retaining 89.9 ± 1.1% of its initial activity after 24 h, while ApCA and DvCA8.0 retained 85.1 ± 1.4% and 90.4 ± 1.3%, respectively (Fig. S2, SI).

To elucidate the contribution of CA in this reaction, it is important to understand the behavior of CO_2 in aqueous media. Gaseous CO_2 can be rapidly dissolved in water to form aqueous $CO_{2\,(aq)}$ with a rate constant of $k_1 = 10^{10}\ s^{-1}$ at 25 °C. However, the hydration of $CO_{2\,(aq)}$ to bicarbonate (HCO_3^-) is considerably slower ($k = 3.6 \times 10^{-2}\ s^{-1}$) under same conditions [16]. Consequently, CO_2 hydration is the rate-limiting step in supplying reactive carbon species ($CO_{2\,(aq)}$ and HCO_3^- in equilibrium) for subsequent conversion to formate in aqueous environments [2]. Under these conditions, all CAs effectively contributed to mitigating the gas–liquid CO_2 transfer limitation by accelerating CO_2 hydration, thereby allowing higher substrate availability in the medium, which resulted in increased CO_2 reduction to formate by FDH. However, the catalytic performance of CAs is not solely determined by their intrinsic activity but is also influenced by mass transfer phenomena within the system. In particular, external mass transfer between the gaseous CO_2 phase and the liquid medium, as well as internal diffusion limitations within immobilized enzyme matrices, may restrict the availability of CO_2 at the enzyme active site [39,44]. Furthermore, reactor hydrodynamics, including agitation intensity, flow rate, and bubble size [45], govern gas–liquid mass transfer and ultimately determine the extent to which CAs can alleviate CO_2 transfer limitations.

Previous studies have shown that immobilized CA can enhance FDH-catalyzed CO_2 reduction to formate, increasing productivity by 1.3–3.6-fold [7,10,46]. This synergy may be a key strategy in CCU applications, enabling more efficient enzymatic CO_2 capture and conversion into value-added products. Based on these results, including stability, catalytic, and immobilization performance, BhCA was selected as the most suitable candidate for the multi-enzymatic system and used in further experiments.

3.2. Engineering a trifunctional biocatalyst with BhCA from cell lysates using a one-step purification and co-immobilization approach

After selecting the optimal CA, immobilization was performed using crude cell lysates as a one-step purification/immobilization strategy. This approach significantly reduces the costs and time associated with enzyme purification [47], enabling the development of more sustainable and cost-efficient biocatalysts. The BhCA amount to be immobilized was estimated from its expression percentage in the lysate (Fig. S3, SI). Table S1 in the SI summarizes the immobilization parameters for both purified and crude preparations, showing that selectivity binding was successfully achieved using crude cell lysates through interactions between the BhCA His-tag residues and the carrier's nickel ions. This affinity binding offers high selectivity, reversibility, and suitability for single-step purification and immobilization [48]. The recovered activity was quite similar in both cases, 38.8 ± 1.7% with purified BhCA and 41.3 ± 1.1% with BhCA from cell lysates.

Subsequently, to determine the maximum binding capacity of Ni^{2+}-ReliZyme for BhCA, different BhCA loadings were evaluated (Table S2, SI). As in the bifunctional biocatalyst previously reported, subsequent washing steps with imidazole and sodium chloride were performed for

this enzyme as well, in order to minimize non-specific protein adsorption onto the carrier at high proteins loadings [24]. BhCA was fully immobilized onto the carrier at loadings up to 10 mg (Table S2, SI). Above this, immobilization yield based on activity slightly declined, suggesting the carrier had reached a plateau, likely due to diffusional limitations reducing substrate accessibility. Reports on other carriers such as iron and titanium nanoparticles have showed maximum BhCA loadings of 8 and 24 mg mL^{-1} [41,49] respectively, highlighting the excellent properties of Ni^{2+}-ReliZyme to accommodate similar amounts of this enzyme. Subsequently, the contribution of different BhCA concentrations on CO_2 reduction by FDH were evaluated. As a result, reducing BhCA loading to 5 and 2 mg g^{-1} (with 10 mg g^{-1} FDH) led to lower formate production, 6.1 ± 0.3 mM and 2.4 ± 0.3 mM, respectively (Fig. S4, SI), demonstrating a concentration-dependent improvement, considering the previous reaction with 10 mg g^{-1} of each BhCA and FDH (Fig. 3). It has been reported that co-immobilization of CA and FDH can sometimes overlap or mask activity [11], however, a 1:1 enzyme ratio of CA:FDH consistently provides high efficiency due to catalytic synchrony [50]. Thus, 10 mg g^{-1} BhCA concentration ensures full retention on the carrier and high catalytic contribution for CO_2 reduction by FDH.

Regarding BhCA co-immobilization with the other two enzymes, the bifunctional biocatalyst developed in a previous work contained ~40 mg g^{-1} GC-GlyDH and 10 mg g^{-1} FDH from crude cells lysate [24]. Since excellent CO_2 reduction to formate was observed with 10 mg g^{-1} each of purified FDH and BhCA (Fig. 3), three GC-GlyDH loadings were tested to determine the optimal enzyme ratio for coordinated activity of all three enzymes, as it is the enzyme in the highest proportion. Fig. 4 shows the recovery activity and immobilization yield of BhCA (fixed at 10 mg g^{-1}) in biocatalysts containing FDH (fixed at 10 mg g^{-1}) and three GC-GlyDH loadings (20, 30, and 40 mg g^{-1}). As observed, BhCA immobilization yield (based on bounded proteins) showed only minor variation, confirming the high surface area of the Ni^{2+}-ReliZyme carrier for accommodating multiple enzymes [51]. Interestingly, BhCA recovered activity increased with higher total protein loading on the carrier (40 mg g^{-1} GC-GlyDH +10 mg g^{-1} FDH), reaching 50.8 ± 2.1%, which exceeded the activity observed when BhCA was immobilized alone (41.3 ± 1.1%). This suggests a more favorable enzyme–carrier interaction, likely due to the reduced density of available functional groups after GlyDH and FDH immobilization, as previously explained. Thus, the trifunctional biocatalyst was prepared by keeping the original GC-GlyDH and FDH loadings (40 and 10 mg g^{-1}, respectively) and adding BhCA at 10 mg g^{-1}. With this ratio, a slight decrease in recovered activity for the other two enzymes was observed compared to the control without BhCA, yielding 2.3 ± 0.4% less for GC-GlyDH and 7.1 ± 0.3% less for FDH, likely due to increased diffusional limitations within the carrier after BhCA incorporation.

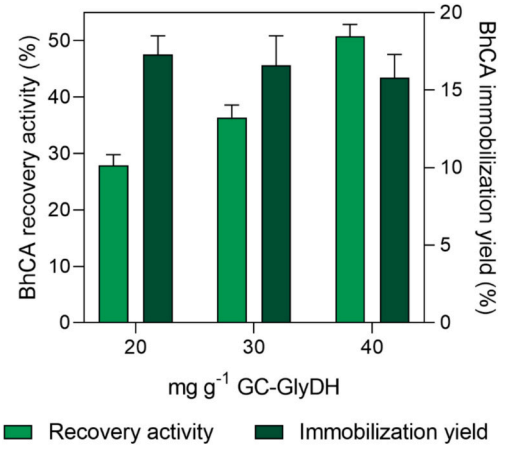

Fig. 4. Recovery activity and immobilization yield (based on bounded proteins) in the co-immobilization of BhCA (10 mg g^{-1}) onto a bifunctional biocatalyst containing a fixed amount of FDH (10 mg g^{-1}) and evaluating three different GC-GlyDH loadings (20, 30, and 40 mg g^{-1}).

Finally, the trifunctional biocatalyst intended for the reaction was prepared. Table 3 summarizes the results for each individual immobilization. Sequential co-immobilization of the three enzymes was successfully achieved with 100% immobilization yields and theoretical activities of 130 ± 1.8, 9.7 ± 0.5, and 34.9 ± 1.9 U g^{-1} for GC-GlyDH, FDH, and BhCA, respectively. As expected, diffusional limitations were detected in the biocatalyst, particularly with GC-GlyDH, which exhibited a lower observed final activity compared to its theoretical activity. It has been reported that GlyDH is highly susceptible to subunit dissociation and destabilization upon immobilization [52]. However, crosslinking with glutaraldehyde has been shown to improve its stability and increase its half-life up to twofold [17]. Nevertheless, the chemical modification induced by glutaraldehyde can cause a significant reduction in activity, up to 50% [24]. Therefore, combined with the diffusional limitations caused by the high protein loading of GlyDH (around 40 mg g^{-1}), the crosslinking effect also reduces its activity but ensures greater retention of its catalytic functions.

Previous studies have demonstrated the successful sequential co-immobilization of multiple enzymes in multi-enzymatic platforms. Li et al. reported a MOF-based biocatalyst incorporating CA, FDH, and glutamate dehydrogenase (GDH) for cofactor regeneration, enabling effective substrate channeling and enhanced CO_2 transfer, which accelerated reaction rates and improved catalytic efficiency [53]. Similarly, Rouf et al. reported a multi-enzymatic platform in which CA, FDH, and GDH were sequentially co-immobilized, resulting in significantly enhanced catalytic efficiency and improved enzyme stability on a hydrophobic support [54]. In addition, this approach allows precise control of enzyme ratios [55] while enabling the use of different immobilization techniques, such as GlyDH crosslinking in this study, without compromising the catalytic integrity of the other enzymes. Overall, sequential co-immobilization has proven to be an effective strategy for orchestrating multi-enzyme systems, providing greater control, higher activity, and improved cascade reaction rates compared with random or simultaneous immobilization [56]. The one-step purification/co-immobilization strategy was successfully implemented, yielding purification factors of 4.3, 2.1, and 5.5 for GC-GlyDH, FDH, and BhCA, respectively. Overall, these results demonstrate the potential of immobilized biocatalysts to enable multi-step reactions through the strategic integration of multiple enzymes on a single carrier.

To further characterize the spatial distribution on the carrier of the three co-immobilized proteins, they were labeled with distinct fluorophores and analyzed by confocal microscopy (Protocol S7, SI). As shown in Fig. 5E, the Ni^{2+}-ReliZyme carrier exhibits a spherical shape with a slightly translucent appearance and no detectable fluorescence at the wavelengths tested. Regarding the individual immobilizations (Fig. 5A, B, and C), the observed fluorescence corresponds to the localization of proteins in the pores near the particle surface, with a similar distribution suggesting a comparable affinity for the carrier. The trifunctional biocatalyst shows an overlap of the red, green, and blue signals, indicating the co-localization of the three enzymes at the same binding sites on the carrier (Fig. 5D). The spatial distribution analysis of

Table 3
Summary of the parameters evaluated in the sequential co-immobilization of GC-GlyDH (coated with glutaraldehyde), FDH and BhCA (from cell lysates) onto Ni^{2+}-ReliZyme carrier.

Parameters	GC-GlyDH	FDH	BhCA
Theoretical biocatalyst activity (U g^{-1})	130 ± 1.8	9.7 ± 0.5	34.9 ± 1.9
Observed biocatalyst activity (U g^{-1})	9.5 ± 0.8	7.9 ± 0.5	32.6 ± 0.5
Yield - Activity (%)	100 ± 0.7	100 ± 0.2	100 ± 0.9
Retained activity (%)	11.0 ± 1.3	80.2 ± 2.5	48.1 ± 2.7
Recovery activity (%)	3.2 ± 0.3	77.7 ± 1.2	46.7 ± 2.3
Bounded proteins (mg g^{-1})	39.1 ± 2.3	10.6 ± 0.6	9.3 ± 1.1
Purification factor	4.3	2.1	5.5

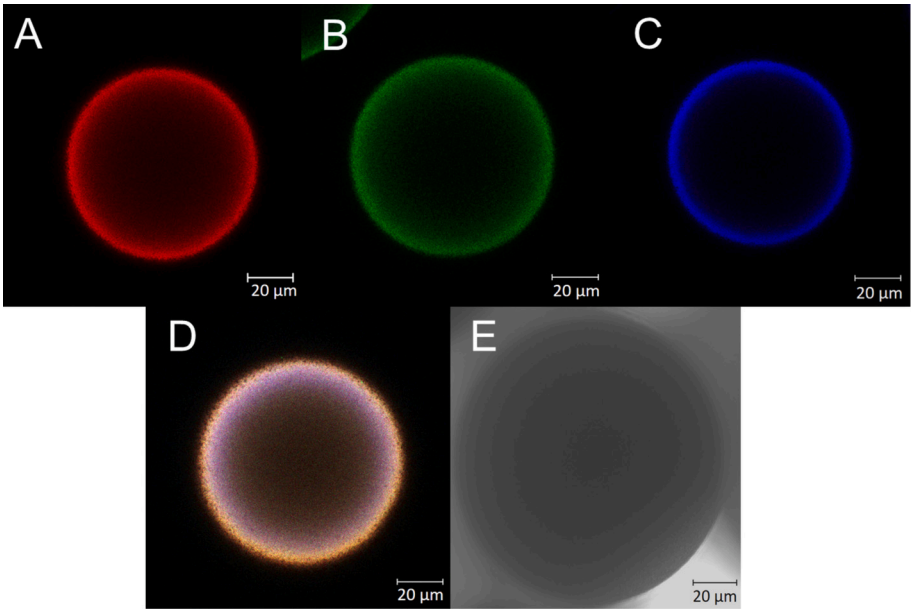

Fig. 5. Compilation of confocal microscopy images of the three individually immobilized proteins and of the trifunctional biocatalyst on Ni^{2+}-ReliZyme carrier. Images were acquired using a Zeiss LSM 980 microscope, with GlyDH, FDH and BhCA labeled with Alexa Fluor™ 610-X, 488 and 405 respectively. Excitation/emission parameters were 603/623 nm, 490/525 nm and 401/422 nm for Alexa Fluor™ 610-X, 488 and 405, respectively. (A) GC-GlyDH. (B) FDH. (C) BhCA. (D) Trifunctional biocatalyst (GC-GlyDH + FDH + BhCA). (D) Ni^{2+}-ReliZyme carrier (control).

the trifunctional biocatalyst reveals a uniform dispersion of the three proteins from the surface into the pores, with GlyDH showing higher intensity within the pores due to its greater loading on the carrier and being the first enzyme immobilized (Fig. S5, SI). These results demonstrate effective co-immobilization, similar distribution, and minimal spatial exclusion, which is critical for multi-enzymatic cascades [57]. The arrangement and proximity of enzymes within co-immobilized biocatalysts play a crucial role in facilitating substrate channeling

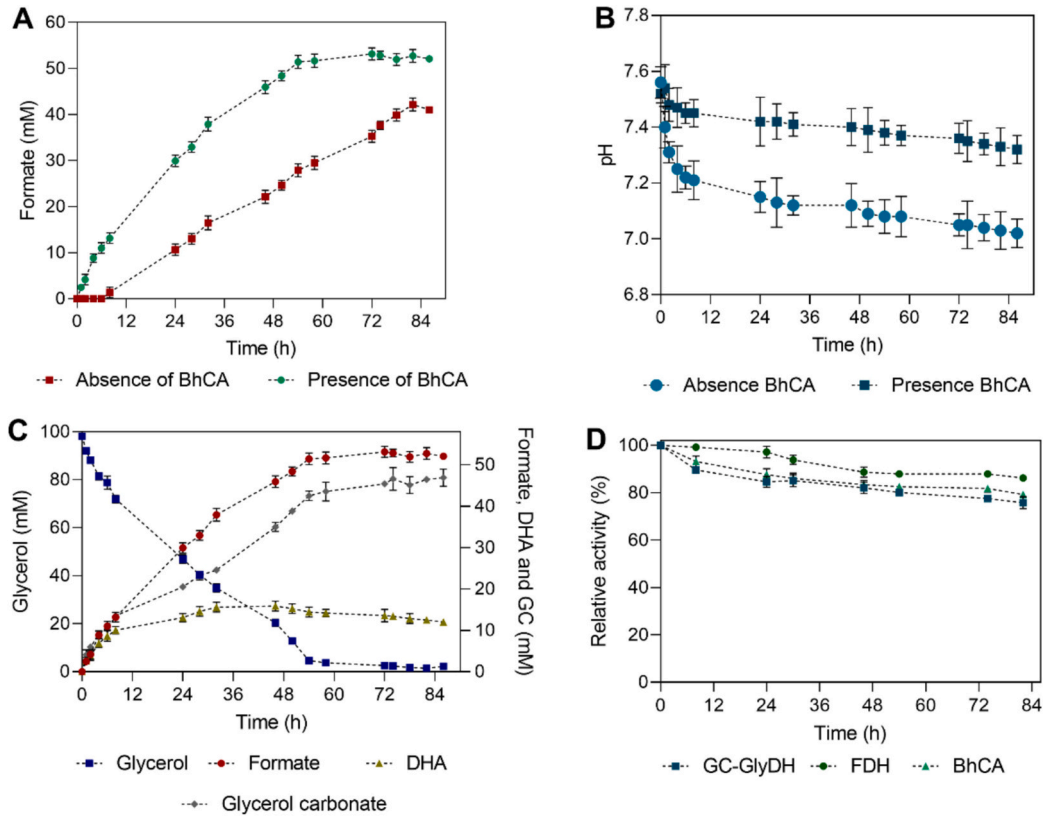

Fig. 6. CA-boosted multi-enzymatic CO_2 conversion into high-value chemicals (formate, DHA and glycerol carbonate). (A) Formate synthesis from CO_2 in the presence and absence of BhCA. (B) pH during the reaction in the absence and presence of BhCA. (C) Time-course of the BhCA-enhanced multi-enzymatic CO_2 reduction to value-added products. (D) Operational stability of the co-immobilized trifunctional biocatalyst.

(including cofactors) while minimizing protein clustering on the carrier [58]. This ensures uniform catalytic activity throughout the particle, which has been shown to improve the performance of cascade reactions and metabolic pathways [59].

3.3. Carbonic anhydrase-boosted multi-enzymatic CO_2 conversion into high-value chemicals

The multi-enzymatic conversion of CO_2 into value-added products was performed in a 200 mL volume using the trifunctional biocatalyst and a gas flow rate of 0.1 vvm from a 20% CO_2 mixture. The gas flow rate for this system was previously optimized using a 24% CO_2 gas mixture, based on pH-driven CO_2 speciation, which led to improved biocatalyst operational stability and maximized utilization of the captured CO_2 when operating at a low flow rate of 0.1 vvm and near-neutral pH (7.1–7.3) [25]. Fig. 6 summarizes the main results, including time course, pH over time, biocatalyst operational stability and the control reaction without BhCA used to evaluate its contribution to the system. The full time-course of this control reaction is illustrated in Fig. S6, SI. BhCA presence markedly enhanced formate synthesis by FDH, increasing the reaction rate from 0.54 to 2.34 mM h^{-1}, representing a 4.3-fold improvement compared to control reaction (Fig. 6 A). This acceleration of the reaction led both to a higher formate concentration (51.4 ± 1.4 mM vs. 42.2 ± 1.1 mM in the control) and a reduced reaction time to reach maximum formate production (from 82 to 54 h). Likewise, the formate productivity increased from 23.2 ± 1.3 to 42.9 ± 0.8 mg L^{-1} h^{-1}, representing a 1.8-fold improvement (Table S4, SI).

Some reports have documented that immobilized CA can significantly enhance CO_2 conversion by FDH. In a bio-electrochemical system, CA increased formate production 1.3-fold with a co-immobilized FDH + CA biocatalyst by enabling rapid CO_2 dissolution [11]. On the other hand, CA and FDH cross-linked using microbial transglutaminase (MTG) exhibited a 3.6-fold increase in catalytic efficiency for formate production when co-immobilized in the same proportion [50]. The synergy of CA and FDH is a well-established strategy, as their proximity on the carrier enables efficient CO_2 adsorption and higher conversion to formate [54,60].

The synergistic mechanism between CA and FDH involves the fact that, despite constant gas supplementation, CO_2 transfer from the gas phase to the liquid medium remains a limiting factor, with pH playing a crucial role. As shown in Fig. 6 B, the pH in the reaction without BhCA decreases slightly from 7.5 to 7.0 due to proton (H^+) generation caused by the slow CO_2 hydration at this low volumetric flow rate (0.1 vvm). However, when BhCA is added, this pH drop is less pronounced (from 7.5 to 7.3), reflecting an improved interconversion between CO_2 and bicarbonate species by the CO_2 hydration catalyzed by the BhCA. Although formate production may be more favorable at lower pH, where the equilibrium CO_2 concentration is higher [61], the pH range observed during this reaction indicates a predominance of bicarbonate and less CO_2 in equilibrium (as observed in Fig. S7, SI), which could be contradictory. To explain this, Fig. 7 presents a scheme of the CO_2 capture and utilization system using the enzymes CA and FDH, according to the findings by Sato and Amao [7]. CA-mediated enhancement of CO_2 gas–liquid mass transfer, through its hydration to bicarbonate, occurs at neutral pH, in agreement with previous observations. Although certain studies have reported formate production from bicarbonate by FDH [62,63], the underlying mechanism remains ambiguous, since other investigations have provided evidence that FDH from *Candida boidinii* (CbFDH) exclusively recognizes CO_2 as its substrate [64,65]. Therefore, the contribution of CA lies in maintaining optimal dissolved CO_2 concentrations by accelerating the establishment of a more efficient dynamic equilibrium between CO_2 and bicarbonate species. This equilibrium is re-established rapidly each time CO_2 is consumed by FDH for formate production, resulting in a moderated pH decrease due to CA's catalytic action [10]. This highlights CA-assisted CO_2 capture as a key enzymatic synergy strategy for developing more efficient

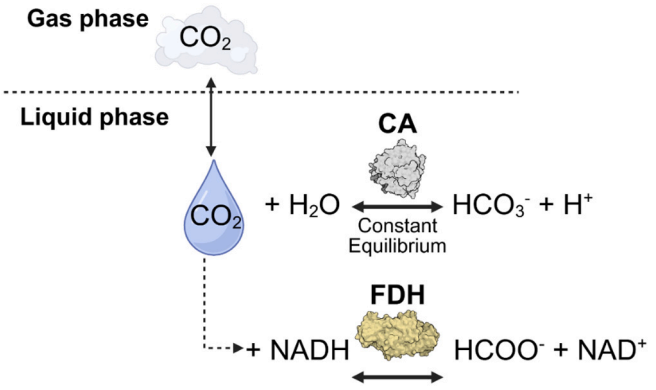

Fig. 7. CO_2 capture and utilization enzymatic system using CA and CbFDH. Schematic adapted from Sato and Amao [7].

biocatalytic CO_2 transformation processes.

As shown in Fig. 6 A, formate was only detected after 8 h in the control reaction without BhCA. However, the contribution of BhCA enabled formate production as early as 1 h due to the higher reaction rate, effectively eliminating the initial asynchronous formation between formate and DHA previously observed in the free-enzyme system [23]. Regarding DHA, its adsorption onto the biocatalyst has been previously reported by the authors due to interactions between amino groups of immobilized proteins and DHA via the Maillard reaction [17], resulting in an adsorption capacity of 140.8 mg DHA g^{-1} biocatalyst [24]. Consequently, only a fraction of the synthesized DHA is detected in the liquid phase considering the equimolar production with formate. During the first 8 h, DHA production followed a similar trend to formate but later plateaued due to adsorption (Fig. 6 C). After 54 h, DHA reached 14.4 ± 1.2 mM, significantly higher than in the control reaction, 4.7 ± 0.4 mM (Fig. S6, SI), suggesting a possible shift in DHA adsorption equilibrium driven by the faster co-production rate facilitated by BhCA. However, further studies are needed to clarify how these conditions affect DHA adsorption onto this material.

Concerning glycerol carbonate (GC), its synthesis has been previously reported in this system as a side reaction between CO_2 and glycerol catalyzed by metals [66], in this case the nickel (Ni^{2+}) from the functionalized-ReliZyme carrier and zinc (Zn^{2+}) from the metalloenzyme GlyDH from *Bacillus stearothermophilus* used in this study, as previously reported by the authors [23,24]. Although BhCA is also a zinc-containing metalloenzyme (structure in Fig. S8, SI) [28], no significant improvement was observed for this metal-catalyzed reaction, suggesting that the beneficial effect was more closely related to the contribution of formate production by FDH rather than to GC synthesis under these conditions. However, GC synthesis provides an alternative route for CO_2 and glycerol valorization in this system, enhancing process sustainability through the production of another industrially relevant product while maximizing substrate utilization. Furthermore, our previous study demonstrated that the biocatalyst prepared via an affinity-based strategy (Ni^{2+}–His-tag) exhibited high robustness and stability, along with reduced substrate inhibition of GlyDH by DHA [24], making the synthesis of GC an inherent feature of the system due to the presence of Ni^{2+}.

According to the biocatalyst's operational stability (Fig. 6 D), three enzymes remained highly stable, with more pronounced inactivation during the first 32 h, coinciding with the peak reaction rate and productivity. After 54 h, residual activities were 75.8 ± 1.1%, 86.2 ± 1.2%, and 82.6 ± 1.3% for GC-GlyDH, FDH, and BhCA, respectively. Compared to the control reaction, activity losses of 5.3% and 7.7% for GC-GlyDH and FDH likely resulted from a higher inactivation under the accelerated conditions with BhCA. For immobilized BhCA, some reports have shown high operational stability in continuous CO_2 capture and mineralization, retaining up to 50% activity for 20 days [35,41],

highlighting its potential for industrial use in immobilized multi-enzymatic CCU systems. As a result, combining an appropriate CO_2 supply with BhCA-assisted CO_2 gas-liquid mass transfer led to an improvement in the catalytic efficiency and maintains a stable neutral pH, essential for CO_2 conversion [7] and the proper functioning of FDH and GlyDH enzymes.

3.4. Long-term operational performance of BhCA in the multi-enzymatic CO_2 conversion system

To assess BhCA's robustness and its contribution on target product yields, the reusability of the trifunctional biocatalyst was tested over five consecutive cycles. Fig. 8 shows the product yields and biocatalyst stability across these cycles. Notably, formate synthesis remained high at 80.3 ± 1.9% after five cycles, corresponding to 298 h of continuous operation (Fig. 8 A). The yield dropped sharply from 100% to 92.1% in the second cycle, but the decline was less pronounced in subsequent cycles, suggesting that a plateau had been reached. Remarkably, the final formate concentration in the fifth cycle was 1.5 times higher than in a single cycle without BhCA, highlighting the enzyme's robust and sustained role in boosting CO_2 reduction by FDH over multiple cycles. As shown in Fig. 8 B, BhCA maintained 63.5 ± 0.8% activity after five cycles, demonstrating excellent operational stability. Inactivation was more pronounced after the second and third cycles, but from the fourth cycle onward, activity stabilized, suggesting a plateau had been reached. These results suggest that the BhCA may also reach a conformational equilibrium, adopting a stable form with functional sites that are less susceptible to inactivation [67], as previously observed with GC-GlyDH and FDH in the previous bifunctional biocatalyst [24].

Several studies have shown the robustness of immobilized CA in diverse CO_2 capture processes. During mineralization, CA immobilized on zinc nanoparticles, as well as on biopolymer matrices retained over 85.4% and 50% of its initial activity, respectively, after at least five consecutive cycles [6,17]. In studies on CO_2 adsorption in solvent systems, CA immobilized on magnetic MOFs showed notable stability, retaining 64% and 54.2% of its activity after six and four consecutive cycles, respectively [68,69]. These findings highlight the high operational stability of immobilized CA, supporting its potential as a robust biocatalyst across diverse industrial applications.

For the other two enzymes, residual activity was 68.3 ± 0.6% for GC-GlyDH and 74.9 ± 1.1% for FDH after five cycles (Fig. 8 B), with a plateau reached from the second cycle for GC-GlyDH and the fourth for FDH, in line with the findings reported in a previous work [24]. The high operational stability of both enzymes was expected, as they tend to be more stable under near-neutral pH conditions with lower CO_2 supply (0.1 vvm), as reported previously [25].

For the other products, DHA gradually increased as the biocatalyst became saturated over the cycles (Fig. 8 A), leading to greater accumulation in the liquid phase. By the fifth cycle, DHA production was 20.8 ± 0.4 mM, representing the 50.4% of the total produced based on the equimolar formate synthesis. This suggests that DHA concentration in the liquid phase would likely increase in subsequent cycles due to adsorbent saturation. Table S3 in the SI presents a mass balance of DHA adsorbed over the reaction cycles, resulting in a total of 2440.2 ± 2.9 mg of adsorbed DHA and corresponding to an adsorption capacity of 126.2 mg DHA g^{-1} biocatalyst. Compared with the estimated maximum capacity (140.8 mg DHA g^{-1}), this result indicates that the biocatalyst is close to full saturation. Moreover, this effect could be further enhanced by the presence of a third enzyme, which may increase DHA interactions with the amine groups in the biocatalyst.

Regarding GC, a consistent production across cycles was observed, with yields above 94.9 ± 2.3% (Fig. 8 A). These findings indicate that enzyme inactivation has a negligible impact on the GC synthesis under the studied conditions. Moreover, it suggests that nickel, which plays the predominant role in driving the reaction, retains its catalytic stability throughout the process, showing minimal degradation consistent with previous reports [70,71].

Table S4 in the SI summarizes the performance metrics results from the evaluated reaction cycles, including space-time yield (STY), specific productivity, and catalyst yield. For formate production, the cumulative STY reached 36.4 mg L^{-1} h^{-1}, representing a 1.6-fold improvement over our previous study conducted under similar conditions but without BhCA and with a higher CO_2 flow rate (1 vvm) [24,16] underscoring the crucial role of immobilized BhCA in contributing to CO_2 utilization efficiency within immobilized multi-enzymatic systems. For DHA and GC, the cSTY values were 27.7 and 87 mg L^{-1} h^{-1}, representing 1.7-fold and 1.5-fold improvements, respectively [24]. This beneficial effect was also reflected in the catalyst yield for each product, demonstrating the enhanced catalytic performance achieved through BhCA contribution in the immobilized multi-enzymatic system.

The enzymatic production of these compounds has been widely explored in the literature, reaching productivities similar to or lower than those reported in our system. Li et al. reported a tri-enzymatic biocatalyst in MOFs containing FDH and CA for the production of formic acid with cofactor regeneration, showing high operational stability after 10 cycles (86%); however, it exhibited a lower formate STY (~21.2 mg L^{-1} h^{-1}) at a smaller reaction scale [53]. In contrast, Rouf et al. reported a remarkable formate productivity in a multi-enzymatic system, in which CA and the hydrophobic nature of MOFs synergistically enhanced the local availability of CO_2 [54]. On the other hand, Zhang et al. reported a lower formate productivity (0.025 mg L^{-1} h^{-1}) using an MTG-cross-linked biocatalyst based on FDH and CA aggregates [50]. Notably, other studies have also documented that CA functions as a significant booster of FDH-mediated formate synthesis, intensifying production rates even beyond those of electro- and photoenzymatic hybrid systems [11,46].

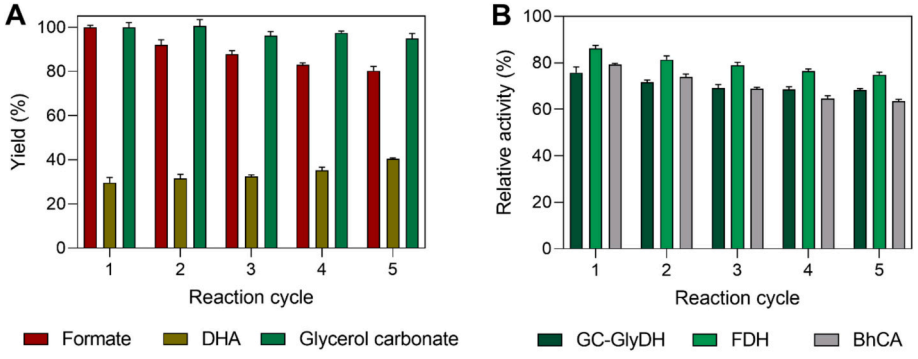

Fig. 8. Robustness of the multi-enzymatic CO_2 reduction assisted by BhCA, evaluated through the trifunctional biocatalyst reusability over five consecutive reaction cycles. (A) Yield of each product in each reaction cycle. (B) Operational stability of the trifunctional biocatalyst in each reaction cycle. Yields and residual activity from the first cycle at the initial reaction time were defined as the 100% reference values.

For DHA, this platform achieved a productivity comparable to that reported by Tack Oh et al., using a hydrogel bioreactor with GlyDH immobilized on silica nanoparticles and reaching an STY of ~21 mg L^{-1} h^{-1} [72]. In addition, DHA productivity in the final reaction cycle was slightly higher than that of other GlyDH-immobilized systems using materials such as mesoporous silica and sepharose, due to the contribution of BhCA in the multi-enzymatic co-production with formate [73,74]. For glycerol carbonate (GC), the highest productivities are obtained under high temperature and pressure via transesterification catalyzed by metals such as nickel and through conversion from inorganic compounds, reaching STY up to 2.7 kg L^{-1} h^{-1} and yields above 58% [75,76]. However, synthesizing GC under mild conditions enhances the sustainability of this multi-enzymatic system while enabling CO_2 valorization to produce this compound.

Compared with most previously reported CCU systems employing CA, which primarily exploit its catalytic activity to accelerate CO_2 hydration, the present study expands its application toward an integrated multi-enzymatic platform capable of simultaneously improving CO_2 utilization, coupling cofactor regeneration and multi-product synthesis, and maintaining high long-term operational stability under industrially relevant conditions. As a result, CA was clearly identified as a key factor in improving the efficiency and productivity of the multi-enzymatic CO_2 reduction system, driving higher reaction rates and greater product yields through enhanced CO_2 gas–liquid mass transfer.

Despite these findings, larger-scale studies would be useful to determine the industrial potential and techno-economic feasibility of this system, including energy demand, production costs, market price of the products and downstream requirements. This study, however, addresses key aspects such as the development of a biocatalyst from crude cell lysates with excellent reusability over multiple reaction cycles, potentially reducing associated costs. In addition, the system operates under mild conditions, and the yields obtained for a portfolio of compounds enable the valorization of industrial feedstocks. In our previous work, the system demonstrated complete CO_2 capture and conversion under these conditions, a low environmental impact in terms of climate change [25], and straightforward isolation of one of the products, formate, via liquid–liquid extraction using a green solvent [23]. Together, these bench-scale results provide a strong foundation for further scale-up studies aiming to address the techno-economic analyses of this bioprocess.

4. Conclusions

The contribution of CA was successfully demonstrated in the CO_2 reduction to formate within a multi-enzyme CCU system for the co-production of high-value compounds. Each CAs screened showed excellent performance, with BhCA identified as the optimal candidate for the system based on its catalytic efficiency and immobilization. Despite some activity loss upon immobilization on Ni^{2+}-ReliZyme due to its high density of functional groups, co-immobilization of BhCA with FDH showed a strong synergy, achieving 97.7% CO_2 conversion on formate (based on NADH consumption) and high BhCA operational stability (89.6 ± 0.8%). Based on these results, a trifunctional biocatalyst containing BhCA was rationally prepared and optimized according to the original mass ratio of GC-GlyDH and FDH using crude cell lysates, resulting in improved carrier interactions due to a lower density of functional groups and enhanced BhCA activity. In the multi-enzymatic CO_2 reduction system, BhCA boosted FDH-mediated formate production, increasing productivity by 1.8-fold and accelerating the reaction rate by 4.3-fold. This synergy led to improvements in both gas–liquid CO_2 transfer and subsequent CO_2–bicarbonate interconversion at neutral pH, resulting in greater CO_2 utilization, overall reaction efficiency and products yields. BhCA also demonstrated high robustness over five consecutive cycles, retaining 63.5 ± 0.8% of its activity and achieving a formate yield of 80.3 ± 1.9%. As a result, BhCA represents a valuable biocatalyst for the intensification of bio-based CCU processes, boosting efficient CO_2 capture and its subsequent conversion into high-value compounds by multi-enzymatic platforms.

CRediT authorship contribution statement

Sady Roberto Rodriguez: Writing – review & editing, Writing – original draft, Methodology, Investigation, Formal analysis, Conceptualization. **Ayanne De Oliveira Maciel:** Writing – review & editing, Investigation, Formal analysis. **Oscar Romero:** Writing – review & editing, Visualization, Validation, Supervision, Methodology, Funding acquisition. **Marina Guillén:** Writing – review & editing, Visualization, Validation, Supervision, Methodology, Funding acquisition. **Io Antonopoulou:** Writing – review & editing, Validation, Supervision, Resources, Methodology.

Declaration of competing interest

The authors declare that they have no known competing financial interests or personal relationships that could have appeared to influence the work reported in this paper.

Acknowledgments

S.R.R. acknowledges the Generalitat of Catalunya (AGAUR) for his pre-doctoral scholarship (Joan Oro – 2022FI_B 00955). S.R.R. also acknowledges the Erasmus+ Programme of the European Union S.R.R., O. R and M.G. acknowledge Generalitat de Catalunya, and the 2021 SGR 00143 and project MEPLABCO$_2$ (TED2021-129732 A-I00) funded by MCIN/AEI/10.13039/501100011033 and by the European Union "NextGenerationEU"/PRTR. This paper is based upon work from COST Action COZYME CA21162, supported by COST (European Cooperation in Science and Technology) facilitating a collaboration between Universitat Autònoma de Barcelona and Luleå University of Technology.

Appendix A. Supplementary data

Supplementary data to this article can be found online at https://doi.org/10.1016/j.cej.2026.177653.

Data availability

Research Link Provided

Replication data for "Carbonic anhydrase boosts multi-step CO2 conversion: A synergistic approach of co-immobilized enzymes for CO2 valorization" (Original data) (CORA)

References

[1] O. Awogbemi, D.V. Von Kallon, Towards the development of underutilized renewable energy resources in achieving carbon neutrality, Fuel Communications 17 (2023) 100099, https://doi.org/10.1016/j.jfueco.2023.100099.
[2] S. Talekar, B.H. Jo, J.S. Dordick, J. Kim, Carbonic anhydrase for CO_2 capture, conversion and utilization, Curr. Opin. Biotechnol. 74 (2022) 230–240, https://doi.org/10.1016/j.copbio.2021.12.003.
[3] Y. Jiang, Z. Ma, Z. Gu, F. Liu, P. Shen, C.S. Poon, A novel approach for improving aqueous carbonation kinetics with CO_2 micro- and nano-bubbles, Chem. Eng. J. 500 (2024) 157363, https://doi.org/10.1016/j.cej.2024.157363.
[4] C.T. Supuran, Carbonic anhydrases, in: Metalloenzymes, Elsevier, 2024, pp. 139–156, https://doi.org/10.1016/B978-0-12-823974-2.00014-0.
[5] Y. Shen, P. Shao, J. Zhao, Y. Lu, S. Zhang, Mass Transfer-Reaction Modeling of CO_2 Capture Mediated by Immobilized Carbonic Anhydrase Enzyme on Multiscale Supporting Structures, Environ. Sci. Technol. 59 (4) (2025) 1995–2005, https://doi.org/10.1021/acs.est.4c09673.
[6] A. Sharma, A. Bhattacharya, A. Shrivastava, Biomimetic CO_2 sequestration using purified carbonic anhydrase from indigenous bacterial strains immobilized on biopolymeric materials, Enzym. Microb. Technol. 48 (4–5) (2011) 416–426, https://doi.org/10.1016/j.enzmictec.2011.02.001.
[7] R. Sato, Y. Amao, Carbonic anhydrase/formate dehydrogenase bienzymatic system for CO_2 capture, utilization and storage, React. Chem. Eng. 7 (1) (2022) 181–191, https://doi.org/10.1039/D1RE00405K.

[8] J. Wei, et al., Hollow MOF Immobilized Formate Dehydrogenase and Carbonic Anhydrase for Electroenzymatic CO_2 Reduction, Ind. Eng. Chem. Res. 65 (14) (2026) 7333–7342, https://doi.org/10.1021/acs.iecr.5c04967.

[9] L. Calzadiaz-Ramirez, A.S. Meyer, Formate dehydrogenases for CO_2 utilization, Curr. Opin. Biotechnol. 73 (2022) 95–100, https://doi.org/10.1016/j.copbio.2021.07.011.

[10] Y. Wang, M. Li, Z. Zhao, W. Liu, Effect of carbonic anhydrase on enzymatic conversion of CO_2 to formic acid and optimization of reaction conditions, J. Mol. Catal. B Enzym. 116 (2015) 89–94, https://doi.org/10.1016/j.molcatb.2015.03.014.

[11] S. Srikanth, Y. Alvarez-Gallego, K. Vanbroekhoven, D. Pant, Enzymatic Electrosynthesis of Formic Acid through Carbon Dioxide Reduction in a Bioelectrochemical System: Effect of Immobilization and Carbonic Anhydrase Addition, Chem Phys Chem 18 (22) (2017) 3174–3181, https://doi.org/10.1002/cphc.201700017.

[12] Y. He, Y. Li, J. Liu, L. Su, C. Du, W. Yuan, The synergistic effect of formate dehydrogenase and carbonic anhydrase accelerates the ethanol fermentation process and improves carbon recovery, Green Chem. 27 (23) (2025) 6776–6786, https://doi.org/10.1039/D5GC00705D.

[13] R. Villa, S. Nieto, A. Donaire, P. Lozano, Direct Biocatalytic Processes for CO_2 Capture as a Green Tool to Produce Value-Added Chemicals, Molecules 28 (14) (2023) 5520, https://doi.org/10.3390/molecules28145520.

[14] A. de Oliveira Maciel, P. Christakopoulos, U. Rova, I. Antonopoulou, Carbonic anhydrase to boost CO_2 sequestration: Improving carbon capture utilization and storage (CCUS), Chemosphere 299 (2022) 134419, https://doi.org/10.1016/j.chemosphere.2022.134419.

[15] C. Molina-Fernández, P. Luis, Immobilization of carbonic anhydrase for CO_2 capture and its industrial implementation: A review, J. CO_2 Util. 47 (2021) 101475, https://doi.org/10.1016/j.jcou.2021.101475.

[16] C.T. Supuran, Carbonic anhydrase versatility: from pH regulation to CO_2 sensing and metabolism, Front. Mol. Biosci. 10 (2023), https://doi.org/10.3389/fmolb.2023.1326633.

[17] L. Liu, X. Wang, Z. Gao, Y. Zhan, M. Yao, J. Bao, Carbonic Anhydrase Immobilized by ZnO Nanoparticles for Catalytic CO_2 Conversion, Water Air Soil Pollut. 236 (4) (2025) 235, https://doi.org/10.1007/s11270-025-07873-8.

[18] J.K.J. Yong, G.W. Stevens, F. Caruso, S.E. Kentish, The use of carbonic anhydrase to accelerate carbon dioxide capture processes, J. Chem. Technol. Biotechnol. 90 (1) (2015) 3–10, https://doi.org/10.1002/jctb.4502.

[19] M. Groh, E. Lettau, J. Schoknecht, J. Liedtke, L. Lauterbach, S. Leimkühler, Biocatalytic cofactor regeneration for CO_2 reduction: Integration of a hydrogenase and a formate dehydrogenase in H_2-driven systems, J. CO_2 Util. 83 (2024) 102828, https://doi.org/10.1016/j.jcou.2024.102828.

[20] O. Gutiérrez-Sánchez, H.Y.V. Ching, N. Daems, M. Bulut, D. Pant, T. Breugelmans, Bifunctional Artificial Carbonic Anhydrase for the Integrated Capture and Electrochemical Conversion of CO $_2$, ACS Sustain. Chem. Eng. 10 (41) (2022) 13865–13876, https://doi.org/10.1021/acssuschemeng.2c04739.

[21] C. Garcia-Sanz, J.M. Palomo, Zinc Nanobiohybrids for the Photocatalytic Conversion of CO_2 to Bicarbonate, ACS Sustain. Chem. Eng. 12 (36) (2024) 13678–13686, https://doi.org/10.1021/acssuschemeng.4c05893.

[22] J. Yang, et al., Capture and Photocatalytic Conversion of Low-Concentration CO_2 Using a Self-Assembled CdSe @Carbonic Anhydrase Biohybrid System, Chem Sus Chem 18 (15) (2025), https://doi.org/10.1002/cssc.202500856.

[23] S.R. Rodriguez, G. Álvaro, M. Guillén, O. Romero, Multienzymatic Platform for Coupling a CCU Strategy to Waste Valorization: CO_2 from the Iron and Steel Industry and Crude Glycerol from Biodiesel Production, ACS Sustain. Chem. Eng. 13 (4) (2025) 1440–1449, https://doi.org/10.1021/acssuschemeng.4c04908.

[24] S.R. Rodriguez, O. Romero, M. Guillén, Enzyme-Powered CO_2 Utilization: A Bifunctional Immobilized Biocatalyst for Intensified CCU of Industrial Feedstocks to High-Value Chemicals, ACS Sustain. Chem. Eng. 14 (1) (2026) 86–98, https://doi.org/10.1021/acssuschemeng.5c07343.

[25] S.R. Rodriguez, M. Guillén, O. Romero, Enhancing Multi-Enzymatic CO_2 Conversion via Reactor Engineering: Effects of Mass Transfer on Sustainable and Green Metrics, Green Chem. (2026), https://doi.org/10.1039/D6GC00387G.

[26] S. Lukato, G.N. Kasozi, B. Naziriwo, E. Tebandeke, Glycerol carbonylation with CO_2 to form glycerol carbonate: a review of recent developments and challenges, Curr. Res. Green Sustainable Chem. 4 (2021), https://doi.org/10.1016/j.crgsc.2021.100199.

[27] H. Bose, T. Satyanarayana, Utility of thermo-alkali-stable γ-CA from polyextremophilic bacterium Aeribacillus pallidus TSHB1 in biomimetic sequestration of CO_2 and as a virtual peroxidase, Environ. Sci. Pollut. Res. 24 (11) (2017) 10869–10884, https://doi.org/10.1007/s11356-017-8739-5.

[28] S. Faridi, T. Satyanarayana, Novel alkalistable α-carbonic anhydrase from the polyextremophilic bacterium Bacillus halodurans: characteristics and applicability in flue gas CO_2 sequestration, Environ. Sci. Pollut. Res. 23 (15) (2016) 15236–15249, https://doi.org/10.1007/s11356-016-6642-0.

[29] O. Alvizo, et al., Directed evolution of an ultrastable carbonic anhydrase for highly efficient carbon capture from flue gas, Proc. Natl. Acad. Sci. USA 111 (46) (2014) 16436–16441, https://doi.org/10.1073/pnas.1411461111.

[30] A. De Oliveira Maciel, P. Christakopoulos, U. Rova, I. Antonopoulou, Enzyme-accelerated CO_2 capture and storage (CCS) using paper and pulp residues as co-sequestrating agents, RSC Adv. 14 (9) (2024) 6443–6461, https://doi.org/10.1039/D3RA06927C.

[31] I. Antonopoulou, S. Varriale, E. Sapountzaki, A. de Oliveira Maciel, U. Rova, P. Christakopoulos, Directed evolution of an ultrastable carbonic anhydrase from Desulfovibrio vulgaris towards enhanced tolerance to flue gas impurities, Comput. Struct. Biotechnol. J. 27 (2025) 2675–2687, https://doi.org/10.1016/j.csbj.2025.06.007.

[32] I. Antonopoulou, et al., Accelerated carbonate weathering by immobilized recombinant carbonic anhydrase, J. CO_2 Util. 94 (2025) 103050, https://doi.org/10.1016/j.jcou.2025.103050.

[33] R. Murín, et al., The exploitation of a pH-sensitive fluorescent probe for monitoring of carbonic anhydrase activity in vitro under weakly acidic conditions, Chem. Pap. 79 (10) (2025) 7127–7137, https://doi.org/10.1007/s11696-025-04252-9.

[34] J. Santiago-Arcos, S. Velasco-Lozano, F. López-Gallego, Multienzyme Coimmobilization on Triheterofunctional Supports, Biomacromolecules 24 (2) (2023) 929–942, https://doi.org/10.1021/acs.biomac.2c01364.

[35] J. Ali, S. Faridi, A. Kashyap, R. Noori Shabnam, M. Sardar, Surface expression of carbonic anhydrase on E. coli as a sustainable approach for enzymatic CO_2 capture, Enzym. Microb. Technol. 176 (2024) 110422, https://doi.org/10.1016/j.enzmictec.2024.110422.

[36] F. Fonck, H.K. Karlsson, I. Antonopoulou, H. Svensson, Evaluation of enhanced absorption of carbon dioxide using carbonic anhydrase in aqueous solutions of 2-amino-2-methyl-1-propanol, Cleaner Eng. Technol. 25 (2025) 100918, https://doi.org/10.1016/j.clet.2025.100918.

[37] H. Rasouli, I. Iliuta, F. Bougie, A. Garnier, M.C. Iliuta, Enhanced CO_2 capture in packed-bed column bioreactors with immobilized carbonic anhydrase, Chem. Eng. J. 432 (2022) 134029, https://doi.org/10.1016/j.cej.2021.134029.

[38] F. Secundo, Conformational changes of enzymes upon immobilisation, Chem. Soc. Rev. 42 (15) (2013) 6250, https://doi.org/10.1039/c3cs35495d.

[39] X. Zhu, C. Du, B. Gao, B. He, Strategies to improve the mass transfer in the CO_2 capture process using immobilized carbonic anhydrase, J. Environ. Manag. 332 (2023) 117370, https://doi.org/10.1016/j.jenvman.2023.117370.

[40] C. Mateo, et al., Stabilization of Multimeric Enzymes via Immobilization and Further Cross-Linking with Aldehyde-Dextran, in: Immobilization of Enzymes and Cells. Methods in Molecular Biology 2100, Humana, New York, NY, 2020, pp. 175–187, https://doi.org/10.1007/978-1-0716-0215-7_11.

[41] S. Faridi, H. Bose, T. Satyanarayana, Utility of Immobilized Recombinant Carbonic Anhydrase of *Bacillus halodurans* TSLV1 on the Surface of Modified Iron Magnetic Nanoparticles in Carbon Sequestration, Energy Fuel 31 (3) (2017) 3002–3009, https://doi.org/10.1021/acs.energyfuels.6b02777.

[42] P.C. Sahoo, N.S. Sambudi, S. Bin Park, J.H. Lee, J.-I. Han, Immobilization of carbonic anhydrase on modified electrospun Poly(Lactic Acid) membranes: Quest for optimum biocatalytic performance, Catal. Lett. 145 (2) (2015) 519–526, https://doi.org/10.1007/s10562-014-1406-2.

[43] S.S.W. Effendi, C.-Y. Chiu, Y.-K. Chang, I.-S. Ng, Crosslinked on novel nanofibers with thermophilic carbonic anhydrase for carbon dioxide sequestration, Int. J. Biol. Macromol. 152 (2020) 930–938, https://doi.org/10.1016/j.ijbiomac.2019.11.234.

[44] C. Bahamondes, A. Illanes, L. Pouchucq, Effect of external diffusional restrictions in immobilized enzymes in stirred reactors, Biocatal. Biotransform. 43 (3) (2025) 228–244, https://doi.org/10.1080/10242422.2025.2462009.

[45] K.P. Dhaneesh, P. Ranganathan, A comprehensive review on the hydrodynamics, mass transfer and chemical absorption of CO_2 and modelling aspects of rotating packed bed, Sep. Purif. Technol. 295 (2022) 121248, https://doi.org/10.1016/j.seppur.2022.121248.

[46] S. Yu, et al., Light-driven enzymatic nanosystem for highly selective production of formic acid from CO_2, Chem. Eng. J. 420 (2021) 127649, https://doi.org/10.1016/j.cej.2020.127649.

[47] O. Barbosa, C. Ortiz, Á. Berenguer-Murcia, R. Torres, R.C. Rodrigues, R. Fernandez-Lafuente, Strategies for the one-step immobilization–purification of enzymes as industrial biocatalysts, Biotechnol. Adv. 33 (5) (2015) 435–456, https://doi.org/10.1016/j.biotechadv.2015.03.006.

[48] L. Zhou, R. Li, X. Li, Y. Zhang, One-step selective affinity purification and immobilization of His-tagged enzyme by recyclable magnetic nanoparticles, Eng. Life Sci. 21 (6) (2021) 364–373, https://doi.org/10.1002/elsc.202000093.

[49] J. Hou, G. Dong, B. Xiao, C. Malassigne, V. Chen, Preparation of titania based biocatalytic nanoparticles and membranes for CO_2 conversion, J. Mater. Chem. A Mater. 3 (7) (2015) 3332–3342, https://doi.org/10.1039/C4TA05760K.

[50] X. Zhang, W. Shao, B. Chen, M. Wang, Cross-linking of carbonic anhydrase and formate dehydrogenase based on amino acid specific recognition: Conversion of carbon dioxide to formic acid, Enzym. Microb. Technol. 146 (2021) 109763, https://doi.org/10.1016/j.enzmictec.2021.109763.

[51] I. Serra, et al., Developing a novel enzyme immobilization process by activation of epoxy carriers with glucosamine for pharmaceutical and food applications, Catalysts 9 (10) (2019), https://doi.org/10.3390/catal9100843.

[52] C. Fernández-Pizarro, L. Wilson, O. Romero, Catalytic Potential-Guided Design of Multi-Enzymatic System for DHA Production from Glycerol, Processes 12 (9) (2024), https://doi.org/10.3390/pr12092014.

[53] Y. Li, L. Wen, T. Tan, Y. Lv, Sequential Co-immobilization of Enzymes in Metal-Organic Frameworks for Efficient Biocatalytic Conversion of Adsorbed CO_2 to Formate, Front. Bioeng. Biotechnol. 7 (2019), https://doi.org/10.3389/fbioe.2019.00394.

[54] S. Rouf, Y.E. Greish, B. Van der Bruggen, S. Al-Zuhair, A multienzyme system immobilized on surface-modified metal–organic framework for enhanced CO_2 hydrogenation, Carbon Resour. Convers. 7 (4) (2024) 100234, https://doi.org/10.1016/j.crcon.2024.100234.

[55] J. Bié, B. Sepodes, P.C.B. Fernandes, M.H.L. Ribeiro, Enzyme immobilization and co-immobilization: Main framework, advances and some applications, Processes 10 (3) (2022) 494, https://doi.org/10.3390/pr10030494.

[56] K. Xu, X. Chen, R. Zheng, Y. Zheng, Immobilization of Multi-Enzymes on Support Materials for Efficient Biocatalysis, Front. Bioeng. Biotechnol. 8 (2020), https://doi.org/10.3389/fbioe.2020.00660.

[57] S. Kondrat, U. Krauss, E. von Lieres, Enzyme co-localisation: Mechanisms and benefits, Curr. Res. Chem. Biol. 2 (2022) 100031, https://doi.org/10.1016/j.crchbi.2022.100031.
[58] R. Fernandez-Lafuente, Multienzymatic Catalysis and Enzyme Co-Immobilization, Catalysts 13 (12) (2023) 1488, https://doi.org/10.3390/catal13121488.
[59] W. Fan, K. Liang, J. Liang, One-pot spatial engineering of multi-enzymes in metal–organic frameworks for enhanced cascade activity, J. Mater. Chem. A 12 (44) (2024) 30318–30328, https://doi.org/10.1039/D4TA06211F.
[60] M. Chai, A. Razmjou, V. Chen, Metal-organic-framework protected multi-enzyme thin-film for the cascade reduction of CO_2 in a gas-liquid membrane contactor, J. Membr. Sci. 623 (2021) 118986, https://doi.org/10.1016/j.memsci.2020.118986.
[61] H. Choe, et al., Efficient CO_2-reducing activity of NAD-dependent formate dehydrogenase from Thiobacillus sp. KNK65MA for formate production from CO_2 gas, PloS One 9 (7) (2014), https://doi.org/10.1371/journal.pone.0103111.
[62] J. Lee, et al., Molar-scale formate production via enzymatic hydration of industrial off-gases, Nature Chemical Engineering 1 (5) (2024) 354–364, https://doi.org/10.1038/s44286-024-00063-z.
[63] A.S. Aslan, et al., Chaetomium thermophilum formate dehydrogenase has high activity in the reduction of hydrogen carbonate (HCO_3-) to formate, Protein Eng. Des. Sel. 30 (1) (2017) 47–55, https://doi.org/10.1093/protein/gzw062.
[64] R. Sato, Y. Amao, Can formate dehydrogenase from: Candida boidinii catalytically reduce carbon dioxide, bicarbonate, or carbonate to formate? New J. Chem. 44 (28) (2020) 11922–11926, https://doi.org/10.1039/d0nj01183e.
[65] R. Sato, Y. Amao, No competitive inhibition of bicarbonate or carbonate for formate dehydrogenase from *Candida boidinii* -catalyzed CO_2 reduction, New J. Chem. 46 (33) (2022) 15820–15830, https://doi.org/10.1039/D2NJ00575A.
[66] Y.-H. Ke, H. Xu, X. Wang, H. Liu, H. Yuan, Production of glycerol carbonate by coupling glycerol and CO_2 over various metal oxide catalyst, J. CO_2 Util. 83 (2024) 102813, https://doi.org/10.1016/j.jcou.2024.102813.
[67] S. Koide, S. Yokoyama, H. Matsuzawa, T. Miyazawa, T. Ohta, Conformational equilibrium of an enzyme catalytic site in the allosteric transition, Biochemistry 31 (23) (1992) 5362–5368, https://doi.org/10.1021/bi00138a017.
[68] M. Du, H. Chen, J. Ye, S. Zhang, J. Chen, L. Wang, One-pot synthesis of efficient carbonic anhydrase-zeolitic imidazolate framework-8 composite for enhancing CO_2 absorption, J. CO_2 Util. 40 (2020) 101211, https://doi.org/10.1016/j.jcou.2020.101211.
[69] Q. Ying, et al., Core-shell magnetic ZIF-8@Fe_3O_4 -carbonic anhydrase biocatalyst for promoting CO_2 absorption into MDEA solution, J. CO_2 Util. 49 (2021) 101565, https://doi.org/10.1016/j.jcou.2021.101565.
[70] G. Liu, J. Yang, X. Xu, Synthesis of hydrotalcite-type mixed oxide catalysts from waste steel slag for transesterification of glycerol and dimethyl carbonate, Sci. Rep. 10 (1) (2020) 10273, https://doi.org/10.1038/s41598-020-67357-z.
[71] H. Li, et al., Synthesis of glycerol carbonate by direct carbonylation of glycerol with CO_2 over solid catalysts derived from Zn/Al/La and Zn/Al/La/M (M = Li, Mg and Zr) hydrotalcites, Catalysis Science & Technology 5 (2) (2015) 989–1005, https://doi.org/10.1039/C4CY01237B.
[72] W.T. Oh, J. Ham, S. Kim, W.G. Koh, Enzymatic conversion of glycerol to dihydroxyacetone using a hydrogel bioreactor entrapping glycerol dehydrogenase immobilized on silica nanoparticles, Chem. Eng. J. 505 (2025), https://doi.org/10.1016/j.cej.2025.159250.
[73] J. Rocha-Martin, A. Acosta, J. Berenguer, J.M. Guisan, F. Lopez-Gallego, Selective oxidation of glycerol to 1,3-dihydroxyacetone by covalently immobilized glycerol dehydrogenases with higher stability and lower product inhibition, Bioresour. Technol. 170 (2014) 445–453, https://doi.org/10.1016/j.biortech.2014.07.116.
[74] G.S. Kumar, et al., Stabilized glycerol dehydrogenase for the conversion of glycerol to dihydroxyacetone, Chem. Eng. J. 276 (2015) 283–288, https://doi.org/10.1016/j.cej.2015.04.039.
[75] C. Muzyka, S. Renson, B. Grignard, C. Detrembleur, J.M. Monbaliu, Intensified continuous flow process for the scalable production of bio-based glycerol carbonate, Angew. Chem. Int. Ed. 63 (10) (2024), https://doi.org/10.1002/anie.202319060.
[76] J. Jitjamnong, P. Khongprom, T. Ratanawilai, S. Ratanawilai, Glycerol carbonate synthesis *via* transesterification of enriched glycerol and dimethyl carbonate using a Li-incorporated MCM-41 framework, RSC Adv. 14 (9) (2024) 5941–5958, https://doi.org/10.1039/D4RA00290C.